Chain Dynamics in Coronas of Ionomer Aggregates

Zhisheng Gao,† Xing-Fu Zhong, and Adi Eisenberg*

Department of Chemistry, McGill University, 801 Sherbrooke Street West, Montreal, PQ, Canada H3A 2K6

Received June 17, 1993; Revised Manuscript Received August 8, 1993®

ABSTRACT: Chain dynamics in coronas of ionomer aggregates, or the areas surrounding the ionic cores, is reported at the segmental level for poly(styrene-*b*-sodium acrylate) reverse micelles and for sodium carboxylate terminated polystyrene aggregates in CCl_4, on the basis of ^2H NMR measurements. In the synthesis of the ionomers, a short ^2H-labeled styrene block (ca. 3 units) was incorporated into each polystyrene chain. The distances between the ^2H-labeled segments and the ionic cores were controlled by the number of styrene units separating the ^2H-labeled segments from the nonionic–ionic block junctions. NMR line width, signal intensity, and relaxation times of the block ionomers and their nonionic precursors clearly indicate that the mobility of the soluble segments near the ionic cores is reduced dramatically. At a distance of 25 repeat units from the nonionic–ionic block junctions, the mobility is still significantly lower than that in single chains, while at a distance of 50 repeat units from the nonionic–ionic block junction, the mobility is essentially the same as that in the single chains. Even for sodium carboxylate terminated polystyrene, where there is only a single ionic group, the ^2H-labeled styrene segments 14 repeat units away from the nonionic–ionic block junction are still subject to the restriction in mobility imposed by the ionic association. ^2H-labeled ionomers with the same styrene block but different lengths of ionic blocks were also examined; it was found that the longer the ionic block, the slower the motion in the coronas, but the effect becomes less dependent on the ionic block length when the ionic blocks are longer than 6 repeat units. Relaxation data were also obtained at three frequencies (76.75, 46.05, and 30.7 MHz) and at multiple temperatures for $(PS)_{92}$-*b*-$(PS\text{-}d_8)_{4.5}$-*b*-$(PS)_{17}$-*b*-$(PANa)_{15}$ and interpreted by use of the log χ^2 distribution model. The results of the present study support the recently proposed restricted mobility model by Eisenberg, Hird, and Moore for random ionomers, assuming that the effect of ionic association on chain dynamics in polymer melt and in polymer solution is similar in trend.

1. Introduction

When a block copolymer is dissolved in a solvent selectively poor for one of the blocks, the pair interaction between segments of the insoluble block is attractive and the block adopts a collapsed conformation, while for the soluble block, the pair interaction between segments is repulsive and the coil dimension of the block tends to expand. As the block copolymer concentration reaches the critical micelle concentration (CMC), micelles are formed as a result of the intermolecular association between the insoluble blocks. The micellization phenomenon of block copolymers in solutions has been the subject of many studies in recent years, and a number of reviews have also appeared.[1-7]

For block copolymers with relatively short insoluble blocks, spherical micelles are usually observed, with the insoluble blocks in the cores and the soluble blocks in the coronas. Dynamics in micellar cores has been probed by NMR,[8-11] ESR,[12] and fluorescence techniques.[13-15] The micellar cores may be glassy, crystalline, or liquidlike, depending on the segments constituting the insoluble block, the solvent used, and the temperature. The soluble block near the micellar cores is considerably more stretched than free chains of equivalent chain lengths.[2] The soluble block in the corona, or the area surrounding the micellar core, has also been modeled by Gast et al. as a string of blobs with increasing block size at longer radial distances, suggesting higher segment concentration near the interface.[16,17] However, no systematic studies have been reported on the dynamics of the soluble block at the segmental level. It is of great interest to understand the effect of micellization on the dynamics of the soluble segments,[7] especially as a function of the distance from the interface.

In recent years, ion-containing block copolymer micelles have received considerable attention.[5,15,18-26] In the cases of block ionomers, where the shorter blocks are ionic, reverse micelles are formed in organic solvents with low polarities,[20-23] with the ionic blocks in the cores. For poly(styrene-*b*-sodium methacrylate) micelles in toluene, the ionic cores are generally solidlike; however, upon the addition of water, the micellar cores are swollen and become liquidlike, as shown in ^1H, ^2H, ^{23}Na, and ^{17}O NMR measurements.[22,27] In contrast to the studies on dynamics in the ionic cores, no investigations have been reported on mobilities of the soluble blocks in the coronas of ionomer micelles. In the present paper, therefore, the dynamics in the corona region is explored for poly(styrene-*b*-sodium acrylate) in carbon tetrachloride, probed by ^2H NMR. ^2H-labeled styrene segments are located at different distances from the nonionic–ionic block junction.

The understanding of the dynamics of the soluble blocks in block ionomers is also of importance in the fundamental studies of random ionomers.[28-35] It was proposed recently by Eisenberg, Hird, and Moore[35] that the existence of ion pair multiplets in random ionomers reduces the mobility of the polymer chains in their vicinity. As the ion content is increased, the regions of the restricted mobility surrounding each multiplet overlap to form larger continuous regions, resulting in phase-separated behavior. This model provides a satisfactory account for both the dynamic mechanical and the X-ray scattering results. However, no direct observation of the effect of multiplet formation on the mobility of polymer segments in the vicinity of the multiplets has been reported. In the present study, ^2H-labeled block ionomers with only one ionic unit, i.e., sodium carboxylate terminated polystryene ionomers, are also investigated, which provides direct information on the

† Present address: Research Department, Imperial Oil Limited, P.O. Box 3022, Sarnia, Ontario, Canada N7T 7M1.

® Abstract published in *Advance ACS Abstracts*, January 1, 1994.

0024-9297/94/2227-0794$04.50/0

effect of association of ion pairs on the mobility of polymer segments.

The study of mobility in coronas of block copolymer micelles may shed some light on other tethered chain systems.[2] Molecular dynamics simulations on highly branched polymers[36,37] and dendrimers[38,39] have been carried out. An interesting comparison can be made between the present block copolymer systems and the star copolymer systems studied by Daoud and Cotton[40] and by Fetters et al.[41-45] In SANS studies of six-armed polystyrene star block copolymers with deuterated polystyrene blocks either near the core or at the extremities of each arm, it was found that for the star copolymers in toluene, the chains near the cores are somewhat extended due to steric repulsion, but sufficient flexibility is present for the ends of the star arms to behave as random coils.[44] Chain dynamics in poly(amido amine) dendrimers were reported by Meltzer et al., on the basis of ^{13}C and ^{2}H NMR measurements.[46,47] It was concluded that the chain dynamics is insensitive to any possible steric clouding occurring at the molecular surface and that the mobility at interior chain positions decreases with increasing molecular size. However, for dendrimers of the same molecular weight, no dependence of mobility on position along the chain was observed when the ^{2}H-labeled segments were located in the interior. In the studies of grafted and adsorbed polymers on solid surfaces, volume fraction profiles have been obtained either theoretically or experimentally.[48-50] NMR has been used to determine the fraction of polymers bound to the solid surface.[48,49] The highly mobile tails/loops contribute to a "narrow" NMR line, while those segments in trains or near the surface display a "broad" line.

It has also been demonstrated in the studies of surfactants that NMR is a powerful and nonintrusive technique in probing molecular dynamics in colloidal systems.[51] Reverse micelles of Aerosol OT (AOT) were studied by use of ^{13}C NMR in nonpolar solvents,[52,53] and the relaxation data were interpreted either in terms of effective isotropic reorientation correlation times or by using the two-step model of Wennerstrom et al.[54] The mobility of the segments was found to increase gradually from the ionic head group to the terminal methyl group. This approach using ^{13}C NMR cannot be applied to block ionomers systems since different segments in a polymer chain cannot be resolved.

The structure of the block ionomers used in the present study is shown as follows:

	$(PS)_j$-b-$(PS\text{-}d_8)_k$-b-$(PS)_m$-b-$(PANa)_n$ or COONa			
	j	k	m	n
	Block Ionomer			
1	0.0	3.4	74	7.5
2	50	5.0	50	12.5
3	55	2.8	25	9.0
4	74	3.2	20	10.0
5	92	4.5	17	15.0
6	77	3.5	10.8	10.5
7	85	4.1	0.0	9.0
8	61	2.9	14	3.3
9	61	2.9	14	6.4
10	61	2.9	14	14.0
	Sodium Carboxylate Terminated Polystyrene			
1	50	2.5	0.0	1.0
2	28	2.7	28	1.0
3	61	2.9	14	1.0

where PS, PS-d_8, PANa, and COONa stand for polystyrene, perdeuterated polystyrene, poly(sodium acrylate), and sodium carboxylate, respectively, and j, k, m, and n represent the numbers of repeat units in these blocks. The location of the perdeuterated polystyrene block varies from right next to the ionic block ($m = 0$) to the end of the polystyrene block ($j = 0$); thus, the molecular dynamics of the block ionomer micelles can be probed on a segmental level at varying distances from the ionic core. The effect of ionic block length on the mobility of segments in the coronas is also investigated; the number of ionic repeat units ranges from 1 (in sodium carboxylate terminated polystyrene) to 15. For $(PS)_{92}$-b-$(PS\text{-}d_8)_{4.5}$-b-$(PS)_{17}$-b-$(PANa)_{15}$ and its nonionic precursor $(PS)_{92}$-b-$(PS\text{-}d_8)_{4.5}$-b-$(PS)_{17}$-b-$(PtBuA)_{15}$, ^{2}H spin–lattice relaxation measurements were also carried out at multiple field and at a number of temperatures.

Theory

The relaxation of quadrupolar nuclei, such as ^{2}H ($I = 1$), is generally determined by quadrupolar interaction, and thus their relaxation times are directly related to the mobility. The ^{2}H spin–lattice and spin–spin relaxation times are given by[55]

$$T_1^{-1} = (3/10)\pi^2\chi^2[J(\omega_0) + 4J(\omega_0)] \quad (1)$$

$$T_2^{-1} = (3/10)\pi^2\chi^2[(3/2)J(0) + (5/2)J(\omega_0) + J(2\omega_0)] \quad (2)$$

where χ is the deuterium quadrupolar coupling constant, which has been determined from the solid state spectra to be 166 kHz for the samples used in the present study, and $J(\omega)$ is the spectral density function and is defined, for simple isotropic systems, as[55,56]

$$J(\omega) = \tau/(1 + \omega^2\tau^2) \quad (3)$$

ω_0 is the Larmor frequency ($\omega_0 = 2\pi\nu_0$), and τ is the correlation time for molecular tumbling.

For a simple molecule in solution, its tumbling can generally be described by such a single correlation time. However, for macromolecules, more than one type of motion may be involved.[57-65] By use of eqs 1–3, an effective correlation time is obtained which provides information on the average of molecular motions. However, this model may not be able to account for the relaxation data obtained at multiple frequencies.

In order to interpret the multiple frequency NMR relaxation data of polymers in solutions, it was proposed that the segments of polymers in solution undergo many types of isotropic motion with different rates and thus the correlation function is better described by a broad distribution of correlation times instead of just a single one.[66] One successful model was proposed by Schaefer,[66] based on a log χ^2 density function, which describes a broad asymmetric distribution of correlation times. In this model, the spectral density is given by

$$J(\omega) = \int_0^\infty \frac{\tau_0 F(s)(b^s - 1)\,ds}{(b-1)\{1 + \omega^2\tau_0^2[(b^s-1)/(b-1)]^2\}} \quad (4)$$

where τ_0 is the average correlation time and $F(s)$ is the distribution function

$$F(s) = p\Gamma(p)^{-1}(ps)^{p-1}\exp(-ps) \quad (5)$$

p is an adjustable parameter which defines the width of the distribution of correlation times; the larger the p, the narrower the distribution. When the distribution is very narrow, $p > 100$, this model is essentially identical to the single correlation time model. $\Gamma(p)$ is the gamma function of p and serves as a normalization factor. The logarithmic

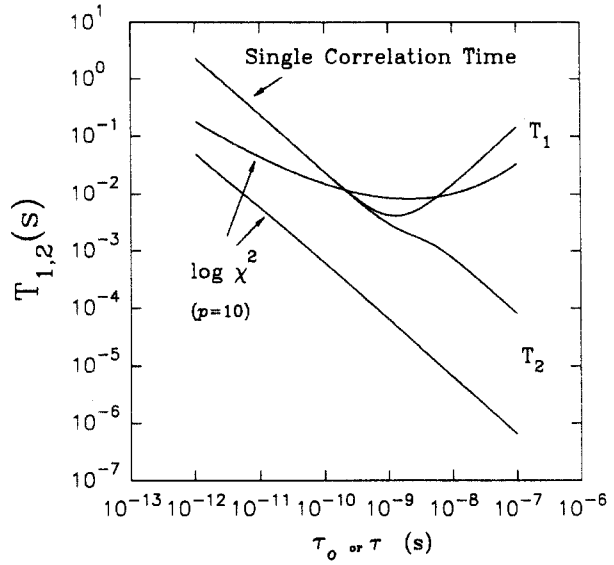

Figure 1. Dependence of spin–lattice and spin–spin relaxation times on the average correlation time of the log χ^2 model (τ_0) and the rotational correlation time of the single correlation time model (τ).

time scale s is defined as

$$s = \log_b [1 + (b - 1)\tau/\tau_0] \quad (6)$$

The logarithmic base b is also an adjustable parameter but is normally fixed at 1000.[66]

The variations of ^{2}H NMR T_1 and T_2 at 76.75 MHz with correlation times in the single correlation time model (τ) and the log χ^2 model (τ_0, p = 10) are given in Figure 1. Clearly, T_1 is a rather complex function of correlation times, while T_2 increases monotonically with an increase in mobility. The relationship between the line width and the apparent spin–spin relaxation time, T_2*, can be expressed as

$$T_2^* = 1/(\pi \Delta\nu_{1/2})$$

where $\Delta\nu_{1/2}$ is the line width at half-height.

Experimental Section

Materials. Perdeuterated styrene monomers (Cambridge Isotope Inc.) were purified by mixing with calcium hydride for 24 h and distilling under vacuum and stored under nitrogen at −20 °C. In order to reduce the loss during the purification process, perdeuterated styrene was usually diluted 10 times with toluene. Before polymerization, it was further treated with fluorenyllithium for 15 min and distilled under vacuum. Styrene (Aldrich) and α-methylstyrene (Aldrich) were also purified using the above method. The purification procedures of *tert*-butyl acrylate (Aldrich), tetrahydrofuran, toluene, *sec*-butyllithium (Aldrich), and LiCl (Aldrich) were the same as described previously.[23] In the preparation of carboxylic acid terminated polystyrene, carbon dioxide gas (Matheson, high purity) was used directly without purification.

Synthesis of ^{2}H-Labeled Block Copolymers. The styrene, perdeuterated styrene, and *tert*-butyl acrylate block copolymers were prepared by the anionic polymerization technique.[23,67] LiCl was first introduced into a previously flamed glass reactor under nitrogen, followed by THF. After the LiCl was dissolved, the solution was cooled to −20 °C, α-methylstyrene and the initiator *sec*-butyllithium were added. The solution was further cooled to −78 °C by dry ice/acetone before the polymerization and then the purified styrene, perdeuterated styrene (10% v/v solution in toluene), styrene, and *tert*-butyl acrylate monomers were introduced sequentially, allowing several minutes for reaction between each addition. In the preparation of carboxylic acid terminated ionomers, carbon dioxide was used instead of *tert*-butyl acrylate. The transfers of these materials to the flask were carried out by use of a syringe or by capillary techniques. The molecular weight and the length of each block were carefully controlled by the amount of initiator and monomers added. An aliquot of the reaction medium was withdrawn for size exclusion chromatography analysis after the reaction of each block was finished. The presence of 5–10 times of excess LiCl was found to be essential in producing block copolymers of very narrow molecular weight distribution. The above procedure not only allows us to prepare poly(styrene-*b*-sodium acrylate) block copolymers having perdeuterated polystyrene segments at different positions along the polystyrene blocks but also the block copolymers with exactly the same styrene and perdeuterated styrene blocks but different lengths of *tert*-butyl acrylate blocks. The block copolymers were recovered by precipitation into methanol and dried under vacuum at 80 °C for more than 24 h. The molecular weight and molecular weight distribution of the polymers were determined using a Varian SEC equipped with a refractometer as detector.

Table 1. Compositions and Molecular Weight Distributions of the ^{2}H-Labeled Block Copolymers Used

compositions	M_w/M_n
$(PS\text{-}d_8)_{3.4}$-*b*-$(PS)_{74}$-*b*-$(PtBuA)_{7.5}$	1.08
$(PS\text{-}d_8)_{3.4}$-*b*-$(PS)_{74}$-*b*-$(PANa)_{7.5}$	1.08
$(PS)_{50}$-*b*-$(PS\text{-}d_8)_5$-*b*-$(PS)_{50}$	1.05
$(PS)_{50}$-*b*-$(PS\text{-}d_8)_5$-*b*-$(PS)_{50}$-*b*-$(PANa)_{12.5}$	1.05
$(PS)_{55}$-*b*-$(PS\text{-}d_8)_{2.8}$-*b*-$(PS)_{25}$-*b*-$(PtBuA)_9$	1.07
$(PS)_{55}$-*b*-$(PS\text{-}d_8)_{2.8}$-*b*-$(PS)_{25}$-*b*-$(PANa)_9$	1.07
$(PS)_{74}$-*b*-$(PS\text{-}d_8)_{3.2}$-*b*-$(PS)_{20}$-*b*-$(PtBuA)_{10}$	1.09
$(PS)_{74}$-*b*-$(PS\text{-}d_8)_{3.2}$-*b*-$(PS)_{20}$-*b*-$(PANa)_{10}$	1.09
$(PS)_{92}$-*b*-$(PS\text{-}d_8)_{4.5}$-*b*-$(PS)_{17}$-*b*-$(PtBuA)_{15}$	1.10
$(PS)_{92}$-*b*-$(PS\text{-}d_8)_{4.5}$-*b*-$(PS)_{17}$-*b*-$(PANa)_{15}$	1.10
$(PS)_{77}$-*b*-$(PS\text{-}d_8)_{3.5}$-*b*-$(PS)_{10.8}$-*b*-$(PtBuA)_{10.5}$	1.05
$(PS)_{77}$-*b*-$(PS\text{-}d_8)_{3.5}$-*b*-$(PS)_{10.8}$-*b*-$(PANa)_{10.5}$	1.05
$(PS)_{85}$-*b*-$(PS\text{-}d_8)_{4.1}$-*b*-$(PtBuA)_{9.0}$	1.09
$(PS)_{85}$-*b*-$(PS\text{-}d_8)_{4.1}$-*b*-$(PANa)_{9.0}$	1.09
$(PS)_{50}$-*b*-$(PS\text{-}d_8)_{2.5}$	1.10
$(PS)_{50}$-*b*-$(PS\text{-}d_8)_{2.5}$-COONa	1.10
$(PS)_{28}$-*b*-$(PS\text{-}d_8)_{2.7}$-*b*-$(PS)_{28}$	1.07
$(PS)_{28}$-*b*-$(PS\text{-}d_8)_{2.7}$-*b*-$(PS)_{28}$-COONa	1.07
$(PS)_{61}$-*b*-$(PS\text{-}d_8)_{2.9}$-*b*-$(PS)_{14}$	1.13
$(PS)_{61}$-*b*-$(PS\text{-}d_8)_{2.9}$-*b*-$(PS)_{14}$-COONa	1.13
$(PS)_{61}$-*b*-$(PS\text{-}d_8)_{2.9}$-*b*-$(PS)_{14}$-*b*-$(PANa)_{3.3}$	1.13
$(PS)_{61}$-*b*-$(PS\text{-}d_8)_{2.9}$-*b*-$(PS)_{14}$-*b*-$(PANa)_{6.4}$	1.13
$(PS)_{61}$-*b*-$(PS\text{-}d_8)_{2.9}$-*b*-$(PS)_{14}$-*b*-$(PANa)_{14}$	1.13

Hydrolysis and Neutralization. The block copolymers were hydrolyzed in toluene to poly(styrene-*b*-perdeuterated styrene-*b*-styrene-*b*-acrylic acid), using *p*-toluenesulfonic acid as catalyst (5 mol % relative to the acrylate content). The solutions were heated at reflux overnight. After cooling, the block copolymers were precipitated in methanol, washed several times with methanol, and then dried under vacuum at 50 °C for at least 24 h. Complete hydrolysis was confirmed by FTIR analysis using a Perkin-Elmer 16PC instrument. The block copolymers in the acid form were converted to the sodium salt form by neutralizing the block copolymers in 2% benzene/methanol 90/10 (v/v) solutions with excess amounts of NaOH. The methanol was stripped off under vacuum, and the polymers were recovered by freeze-drying. The materials were further washed with methanol to remove excess NaOH and then dried under vacuum at 70 °C for at least 24 h. The compositions and molecular weight distributions of the polymers used in the present study are given in Table 1.

NMR Measurements. Clear micellar solutions were prepared by dissolving the neutralized block copolymers directly in carbon tetrachloride (CCl_4). CCl_4 was chosen for the present study since there are no deuterium signals from CCl_4 that may interfere with those from the block copolymers. CCl_4 was purchased from ACP Chemicals (Spectrograde) and used without further purification. Block copolymer solutions, 9.1% (w/w) (1.0 g of polymer in 10.0 g of CCl_4), were used for all the measurements.

^{2}H NMR spectra were recorded at 46.05 MHz on a Varian XL-300 (7.05-T) spectrometer and, to a lesser extent, also at 30.70 and 76.75 MHz on Varian XL-200 (4.70-T) and Varian Unity-500 (11.75-T) spectrometers, respectively. In the measurements of quantitative ^{2}H NMR spectra, 90° pulses (ca. 8 μs) and pulse delays of more than $5T_1$ were used. For convenience,

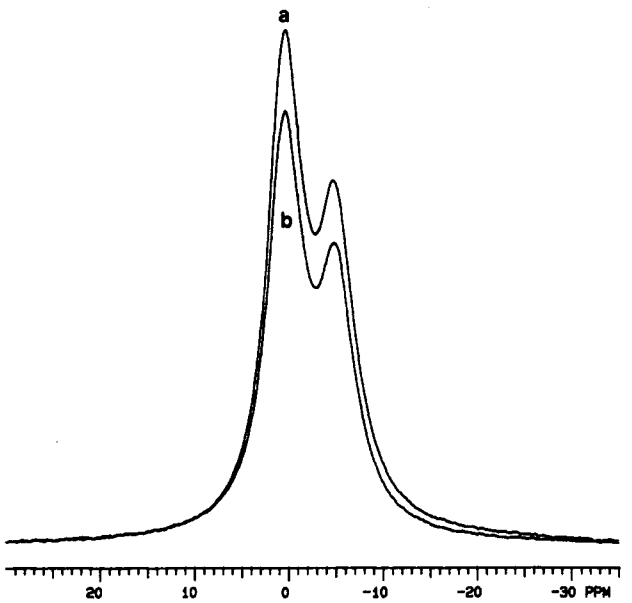

Figure 2. ^{2}H NMR spectra (46.05 MHz) of $(PS)_{50}$-*b*-$(PS\text{-}d_8)_5$-$(PS)_{50}$ (a) and $(PS)_{50}$-*b*-$(PS\text{-}d_8)_5$-*b*-$(PS)_{50}$-*b*-$(PANa)_{12.5}$ (b) in CCl_4 (9.1% (w/w)) at 21 °C.

the aromatic signals were assigned to 0.0 ppm since the present study is not based on chemical shift. Spin–lattice relaxation times were measured using an inverse-recovery pulse sequence, and the line widths were determined by use of a curve fitting procedure. All T_1 values were calculated from peak heights obtained at twelve or more different variable delays, using a nonlinear two-parameter least-squares fitting procedure. Typically, 2000 scans were required to obtain a spectrum. The spin–lattice relaxation times are believed to be reproducible to less than ±3%.

Result and Discussion

Block Ionomers. As discussed in the Theory, the interpretation of the NMR spin–spin relaxation rate is rather straightforward: the shorter the ^{2}H spin–spin relaxation time or the broader the line width, the slower the segmental motion. The ^{2}H NMR spectra of $(PS)_{50}$-*b*-$(PS\text{-}d_8)_5$-$(PS)_{50}$-*b*-$(PANa)_{12.5}$ and $(PS)_{50}$-*b*-$(PS\text{-}d_8)_5$-*b*-$(PS)_{50}$ in CCl_4 (9.1%, w/w) are shown in Figure 2. It should be stressed that the nonionic segments of the two polymers are identical. In the ionomer, the perdeuterated styrene units are located 50 styrene units away from the nonionic–ionic block junction. The ^{2}H line shape of the block ionomer is essentially the same as that of its polystyrene precursor. The small difference in signal intensity is due to the slightly higher molecular weight of the ionomer (both solutions contain 9.1% (w/w) polymers). For $(PS)_{50}$-*b*-$(PS\text{-}d_8)_5$-*b*-$(PS)_{50}$, no micelles are expected to exist in the CCl_4 solution, while the block ionomer is known to form reverse micelles since these have been observed for similar block ionomers in CCl_4, THF, *N*-methylpyrrolidone (NMP), and other solvents.[21-23] The similarity in line shape between the block ionomer and its polystyrene precursor indicates that micelle formation has little effect on the mobility of the styrene segments 50 units from the nonionic–ionic block junction.

When we move the ^{2}H-labeled styrene units closer to the nonionic–ionic block junction, the situation is very different. Figure 3 shows the ^{2}H NMR spectra of $(PS)_{74}$-*b*-$(PS\text{-}d_8)_{3.2}$-*b*-$(PS)_{20}$-*b*-$(PANa)_{10}$ in CCl_4 (9.1%, w/w). Significant line broadening can be observed, indicating that in the micelle, the mobility of the styrene groups 20 units from the nonionic–ionic block junction is slower than those 50 units from the nonionic–ionic block junction. In order to discount the molecular weight effect, the ^{2}H NMR

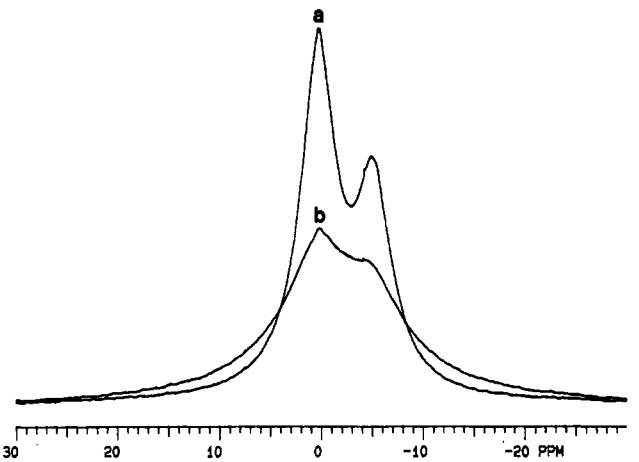

Figure 3. ^{2}H NMR spectra (46.05 MHz) of $(PS)_{74}$-*b*-$(PS\text{-}d_8)_{3.2}$-*b*-$(PS)_{20}$-*b*-$(PtBuA)_{10}$ (a) and $(PS)_{74}$-*b*-$(PS\text{-}d_8)_{3.2}$-*b*-$(PS)_{20}$-*b*-$(PANa)_{10}$ (b) in CCl_4 (9.1% (w/w)) at 21 °C.

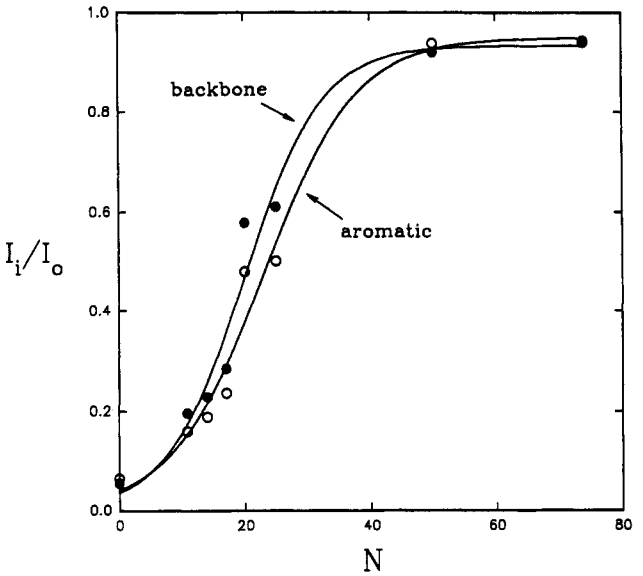

Figure 4. Variations of signal intensity ratios between the block copolymers in the ionic and nonionic forms as a function of the number of styrene units between the deuterated segments and the nonionic–ionic block junction. The data (● backbone, ○ aromatic) were fitted with sigmoidal functions.

spectrum of the block polymer in the *tert*-butyl ester form (i.e., before hydrolysis) is given in Figure 3 for comparison.

In the cases where the ^{2}H-labeled styrene units are even closer to the nonionic–ionic block junctions, the ^{2}H line widths become very broad, and only weak signals can be observed. Although the measurements of line widths become very difficult for these weak signals, information related to the line widths can still be obtained from the signal intensities, since they are directly related to the line widths: the broader the line width, the lower the signal intensity. The ^{2}H NMR intensity ratios between the block ionomers and their nonionic precursors in the ester or polystyrene forms are shown in Figure 4, as a function of the number of styrene units between the nonionic–ionic block junction and the ^{2}H-labeled styrene units. These ratios have been corrected for the molecular weight differences between the block ionomers and their nonionic precursors, since all the measurements were carried out in 9.1% w/w polymer solutions. The decrease in the intensity ratio, corresponding to the broadening of the line width, indicates a decrease in mobility for the ^{2}H-labeled segments.

The intensity ratio of the ^{2}H-labeled segments in the ionic (micellar) form and in the nonionic (single chain)

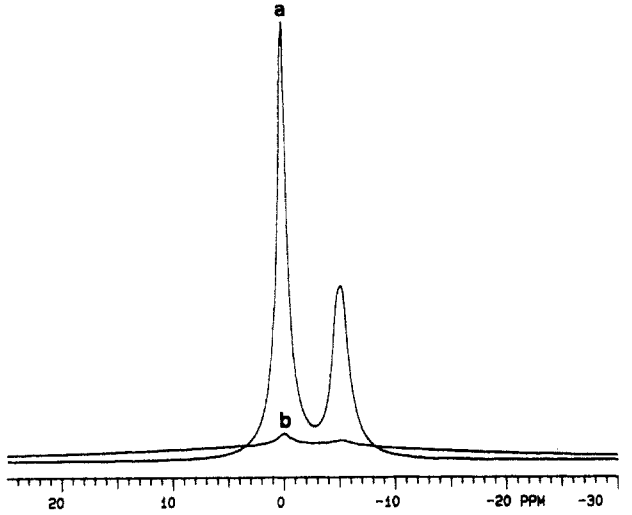

Figure 5. ^{2}H NMR spectra (46.05 MHz) of $(PS)_{50}$-*b*-$(PS\text{-}d_8)_{2.5}$ (a) and $(PS)_{50}$-*b*-$(PS\text{-}d_8)_{2.5}$-COONa (b) in CCl_4 (9.1% (w/w)) at 21 °C.

form appears to follow the sigmoidal function given in eq 7.

$$\frac{I_i}{I_o} = \frac{a0}{1 + \exp\left(-\frac{a1 - N}{a2}\right)} \tag{7}$$

where $a0$, $a1$, and $a2$ are fitting constants, the values of which are

$a0 = 0.95$, $a2 = 23$, $a3 = 7.4$

for the aromatic ^{2}H signals

$a0 = 0.93$, $a2 = 20$, $a2 = 6.2$

for the backbone ^{2}H signals

I_i and I_o are the ^{2}H signal intensities of the block copolymers in the ionic (micellar) and nonionic (single chain) forms, respectively. N is the number of styrene units between the ^{2}H-labeled block and the nonionic–ionic block junction.

It is seen from Figure 4 that the associations between the ionic blocks in the micellar cores affect the mobility of the segments close to the nonionic–ionic block junction significantly. The effect of the micellization decreases as the number of styrene units between the ^{2}H-labeled segments and the nonionic–ionic block junction increases. The influence of ionic interactions on mobility is equally significant for the motions of the phenyl group and the backbone. Our results are consistent with those from the SANS coil dimension study of polystyrene star block copolymers by Lantman et al.[44] It was found that segments near the cores are extended by steric exclusion, but those close to the ends of the star arms behave like random coils.[44]

Sodium Carboxylate Terminated Polystyrene. As mentioned above, the mobility of the styrene segments is highly dependent on the distance from the nonionic–ionic block junction. Furthermore, it is anticipated that the chain dynamics would also depend on the length of the ionic block. In this section, the special case of ionomers with only a single terminal ionic group will be discussed. ^{2}H NMR spectra of $(PS)_{50}$-*b*-$(PS\text{-}d_8)_{2.5}$ and $(PS)_{50}$-*b*-$(PS\text{-}d_8)_{2.5}$-COONa in CCl_4 (9.1%, w/w) are shown in Figure 5. It is obvious that the interactions between the terminal ionic groups lead to a substantial line broadening effect. The mobility of the ^{2}H-labeled styrene units near the ionic groups decreases significantly upon association of the ionic

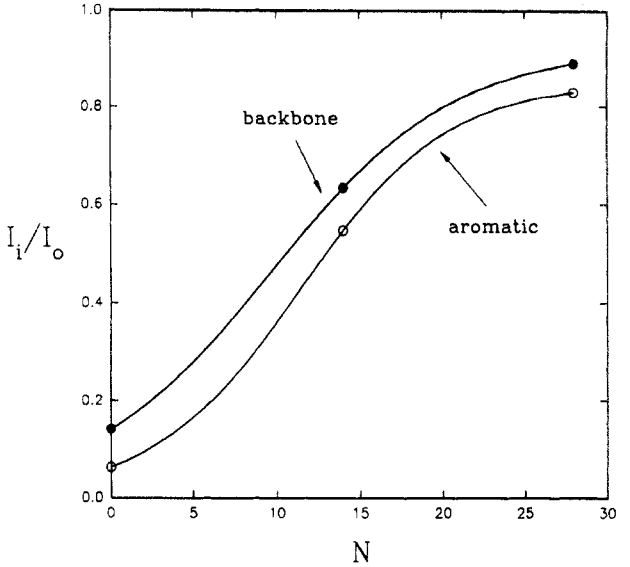

Figure 6. Variations of signal intensity ratios between the sodium carboxylate terminated polystyrene and its polystyrene precursor as a function of the number of styrene units between the deuterated segments and the ionic groups. The data (● backbone, ○ aromatic) were fitted with sigmoidal functions.

groups. The residual ^{2}H signal in $(PS)_{50}$-*b*-$(PS\text{-}d_8)_{2.5}$-COONa is very likely due to the ionomers in the single chain forms. A small amount of $(PS)_{50}$-*b*-$(PS\text{-}d_8)_{2.5}$ may also be present since some of the precursors may have been deactivated before they reacted with CO_2. It should be mentioned that the ^{2}H line widths of $(PS)_{50}$-*b*-$(PS\text{-}d_8)_{2.5}$ are significantly narrower than those of $(PS)_{50}$-*b*-$(PS\text{-}d_8)$-*b*-$(PS)_{50}$ shown in Figure 2. This is due to the fact that the mobility of the styrene segments near the end of the chain is considerably higher than that of styrene segments in the center of the chain.[68]

The dependence of the intensity ratio of the ^{2}H signals from the ionomer and from the polystyrene precursor on the number of styrene units between the ^{2}H-labeled segments and the terminal ionic groups is given in Figure 6. Similar to the results presented in Figure 4, a correction for the molecular weight effect has also been applied. The relationships between the intensity ratio and the number of styrene units separating the ^{2}H-labeled segments from the ionic groups can also be fitted to the sigmoidal function (eq 5 with $a0 = 0.85$, $a1 = 11.4$, and $a2 = 4.47$ for signals from the phenyl group and $a0 = 0.92$, $a1 = 9.6$, and $a2 = 5.6$ for signals from the backbone). It is surprising to observe that the association between the single terminal ionic groups can reduce the mobility of segments more than 20 styrene units away.

These results have significant implications on the fundamental study of random ionomers. It was found from dynamic mechanical studies that, for poly(styrene-*co*-sodium methacrylate) and many other random ionomer systems, a second loss tangent peak appears at ion contents as low as ca. 2 mol %, indicating the formation of clusters with minimum dimensions of 5–10 nm.[69] In a recent model proposed by Eisenberg, Hird, and Moore,[35] the formation of clusters was attributed to the overlapping regions of restricted mobility surrounding individual multiplets. At ionic contents near 5 mol %, the high T_g cluster region becomes dominant, as indicated by the area under the second loss tangent peak.[69] Based on Figure 6, the mobility of the first 10 styrene units from the ionic groups is reduced by at least 50%. It is thus not surprising that for a random polystyrene ionomer above its matrix T_g, the mobilities of the styrene segments between two ionic groups are much

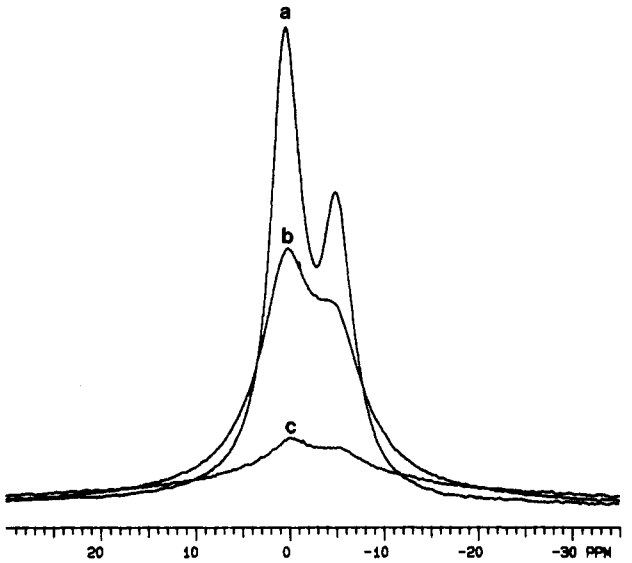

Figure 7. ^{2}H NMR spectra (46.05 MHz) of $(PS)_{61}$-*b*-$(PS\text{-}d_8)_{2.9}$-*b*-$(PS)_{14}$ (a), $(PS)_{61}$-*b*-$(PS\text{-}d_8)_{2.9}$-*b*-$(PS)_{14}$-(COONa) (b), and $(PS)_{61}$-*b*-$(PS\text{-}d_8)_{2.9}$-*b*-$(PS)_{14}$-$(PANa)_{14}$ (c) in CCl_4 (9.1% (w/w)) at 21 °C.

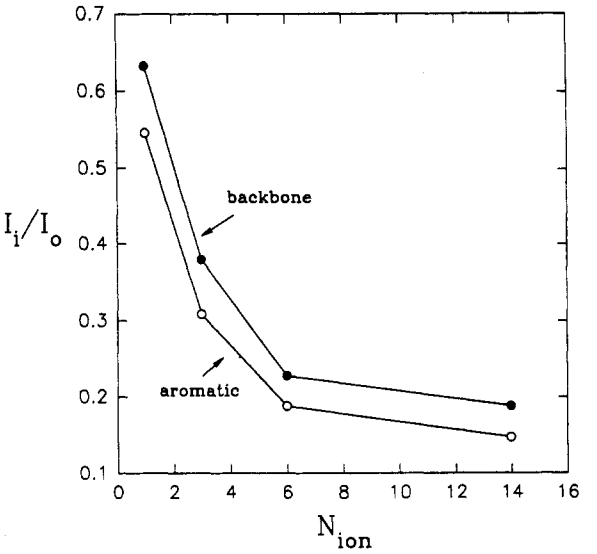

Figure 8. Dependence of signal intensity ratios between the block copolymers in the ionic and nonionic forms as a function of the ionic block length (● backbone, ○ aromatic).

lower than those of the unfunctionalized polystyrene if the distance between two ionic groups is shorter than 20 styrene units. However, one should bear in mind that the multiplet sizes of telechelic ionomers were found to be significantly larger than those of random ionomers,[70] which may affect the mobility in the corona region. Also, the effect of ionic interactions at one end of the polystyrene chain on the mobility of the styrene segments, as studied in the present paper, may be weaker than those of random and telechelic ionomers where ionic interactions occur at both ends. Nevertheless, the present study does prove the existence of a restricted mobility region around the ionic multiplets. Although the present results were obtained from ionomers in solution, it is anticipated that the ionic association has a similar effect on the dynamics of nonionic segments in molten state.

Effect of Ionic Block Length. It is well-known that the aggregation numbers of block copolymer micelles depend significantly on the length of the insoluble blocks.[2] This was also found to be true for block ionomer reverse micelles.[20,21] It is thus of interest to examine the effect of ionic block length on the mobility of ^{2}H-labeled styrene segments at a certain distance from the nonionic–ionic block junction. The ^{2}H NMR spectra of $(PS)_{61}$-*b*-$(PS\text{-}d_8)_{2.9}$-*b*-$(PS)_{14}$, $(PS)_{61}$-*b*-$(PS\text{-}d_8)_{2.9}$-*b*-$(PS)_{14}$-COONa), and $(PS)_{61}$-*b*-$(PS\text{-}d_8)_{2.9}$-*b*-$(PS)_{14}$-*b*-$(PANa)_{14}$ are shown in Figure 7. It is obvious that the line widths of the ^{2}H-labeled styrene segments increase with increasing ionic block length. An increase in ionic block length would lead to the formation of micelles with larger ionic cores and higher aggregation numbers. Both factors are considered to have a significant impact on chain dynamics.

Another possible mechanism responsible for the decrease in mobility is the increase in steric repulsion near the ionic cores. The theoretical value for the radius of micellar cores can be given by[2,71]

$$R_{core} \cong N_B^{1/3} f^{1/3} a \qquad (8)$$

where N_B is the number of repeat units in the insoluble block, f is the aggregation number of the micelles which is known theoretically to be proportional to $N_B^{4/5}$, and a is the size of the repeat unit in the insoluble block. Therefore, in the micellar cores, the total surface area per polymer chain should be proportional to $N_B^{2/5}$, i.e., theoretically, steric repulsion between the soluble segments at the surface of the micellar cores should decrease slightly as the insoluble block length increases. However, it is also anticipated that the average surface area per chain increases with radial distance from the interface, d, at a rate of $(R_{core} + d)^2/R_{core}^2$. The smaller the micellar core, the faster the increase in the average surface area per chain. Therefore, at a certain radial distance from the cores, the average surface area per chain may be lower for block copolymers with longer insoluble blocks, resulting in higher steric repulsion between the soluble blocks of these polymers.

According to the star model, the monomer volume fraction of the soluble block at a certain distance from the micellar center is given by[71]

$$\phi_A(r) = f^{2/3}(a/r)^{4/3} \qquad (9)$$

where r is the distance from the micellar center. Since f is proportional to $N_B^{4/5}$, the monomer volume fraction of the soluble block should increase with increasing insoluble block length. The higher segment density may cause lower mobility. From these theoretical considerations, it is clear that the steric repulsion between the soluble blocks and the higher segmental density near the micellar cores may play an important role here, in addition to the effect that the soluble blocks are attached to heavier micellar cores. Blum et al.[72] have also reported, on the basis of ^{2}H NMR studies, that for selectively deuterated poly(styrene-*b*-2-vinylpyridine) adsorbed on silica surface and reswollen with toluene, the styrene block is extended to approximately 4 times the normal radius of gyration.

The intensity ratios between the ^{2}H signals from the ionomer and those from the polystyrene precursor are given in Figure 8 as a function of the ionic block length. It is of interest to observe that the effect of the ionic block length on the intensity ratio is much more pronounced when the ionic block length is short. When the ionic block length reaches 6, the intensity ratio becomes less sensitive to the ionic block length. This result clearly justifies the presentation in Figure 4 where the ionic block lengths range from 6 to 15.

Analysis of Relaxation Data. The spin–lattice relaxation times of a number of ^{2}H-labeled block ionomers and their nonionic precursors were measured at 46.05 MHz (7.05 T) in CCl_4 solutions (9.1%, w/w), and the results are given in Table 2. For all the nonionic precursors, the spin–

Table 2. Spin–Lattice Relaxation Times Measured at 46.05 MHz (7.05 T) (22 + 1 °C) and Rotational Correlation Times from the Single Correlation Time Model

polymers	aromatic T_1, ms	aromatic τ, ns	aliphatic T_1, ms	aliphatic τ, ns
$(PS)_{77}$-*b*-$(PS\text{-}d_8)_{3.5}$-*b*-$(PS)_{10.8}$-*b*-$(PANa)_{10.5}$	4.93	8.8	4.93	8.8
$(PS)_{61}$-*b*-$(PS\text{-}d_8)_{2.9}$-*b*-$(PS)_{14}$	3.78	6.2	3.90	6.5
$(PS)_{61}$-*b*-$(PS\text{-}d_8)_{2.9}$-*b*-$(PS)_{14}$-COONa	4.39	7.6	4.39	7.6
$(PS)_{61}$-*b*-$(PS\text{-}d_8)_{2.9}$-*b*-$(PS)_{14}$-*b*-$(PANa)_{3.3}$	4.58	8.0	4.67	8.2
$(PS)_{61}$-*b*-$(PS\text{-}d_8)_{2.9}$-*b*-$(PS)_{14}$-*b*-$(PANa)_{14}$	4.82	8.6	4.84	8.6
$(PS)_{92}$-*b*-$(PS\text{-}d_8)_{4.5}$-*b*-$(PS)_{17}$-*b*-$(PANa)_{15}$	4.90	8.7	4.90	8.7
$(PS)_{92}$-*b*-$(PS\text{-}d_8)_{4.5}$-*b*-$(PS)_{17}$-*b*-$(PBtuA)_{15}$	3.80	6.3	3.98	6.7
$(PS)_{74}$-*b*-$(PS\text{-}d_8)_{3.2}$-*b*-$(PS)_{20}$-*b*-$(PANa)_{10}$	4.35	7.5	4.35	7.5
$(PS)_{74}$-*b*-$(PS\text{-}d_8)_{3.2}$-*b*-$(PS)_{20}$-*b*-$(PtBuA)_{10}$	3.95	6.6	3.92	6.6
$(PS)_{55}$-*b*-$(PS\text{-}d_8)_{2.8}$-*b*-$(PS)_{25}$-*b*-$(PtBuA)_9$	3.79	6.3	3.91	6.5
$(PS)_{55}$-*b*-$(PS\text{-}d_8)_{2.8}$-*b*-$(PS)_{25}$-*b*-$(PANa)_9$	4.19	7.2	4.19	7.2
$(PS)_{28}$-*b*-$(PS\text{-}d_8)_{2.7}$-*b*-$(PS)_{28}$	3.78	6.3	3.87	6.5
$(PS)_{28}$-*b*-$(PS\text{-}d_8)_{2.7}$-*b*-$(PS)_{28}$-$(COONa)_9$	4.02	6.8	4.05	6.9

lattice relaxation times are close to 3.90 ms, while for the block ionomers, the spin–lattice relaxation times range from ca. 4.35 to ca. 4.90 ms, depending on the number of styrene units between the ^{2}H-labeled segments and the nonionic–ionic block junctions and the number of sodium acrylate units in the ionic blocks. The closer the ^{2}H-labeled segments to the nonionic–ionic block junction, or the longer the ionic block, the longer the T_1. However, the T_1 of the block ionomers levels off at ca. 4.90 ms. Similar T_1 values were obtained for $(PS)_{61}$-*b*-$(PS\text{-}d_8)_{2.9}$-*b*-$(PS)_{14}$-COONa and $(PS)_{74}$-*b*-$(PS\text{-}d_8)_{3.2}$-*b*-$(PS)_{20}$-*b*-$(PANa)_{10}$, indicating that the mobilities of the ^{2}H-labeled segments are quite similar in these two block ionomer micelles. These results are in very good agreement with those presented in Figures 4 and 6, based on the measurements of signal intensity. Effective correlation times of these block copolymers are given in Table 2, which were calculated by use of the single correlation time model (eq 1–3). The longer correlation times were obtained since the T_1 values at 20–30 °C decrease with increasing temperature (see below).

Multiple-frequency and multiple-temperature relaxation studies were carried out for $(PS)_{92}$-*b*-$(PS\text{-}d_8)_{4.5}$-*b*-$(PS)_{17}$-*b*-$(PtBuA)_{15}$ and $(PS)_{92}$-*b*-$(PS\text{-}d_8)_{4.5}$-*b*-$(PS)_{17}$-*b*-$(PANa)_{15}$ only (Tables 3 and 4). Their spin–lattice relaxation times at 76.75 and 30.7 MHz were measured at 21, 30, 40, 50, 60, and 70 °C (Table 3). The line widths at 76.75 MHz were determined by fitting the spectra with two or more Lorentzian functions. The relationship between spin–spin relaxation times and the line width may not be as simple as that given in eq 8 since the line width of a polymer may be affected by the microstructure of the polymer. Nevertheless, the difference in line width between the block ionomers and their ester precursors can only be attributed to the change in spin–spin relaxation time since the taticities of these two polymers are exactly the same.

The ^{2}H NMR spectrum of $(PS)_{92}$-*b*-$(PS\text{-}d_8)_{4.5}$-*b*-$(PS)_{17}$-*b*-$(PtBuA)_{15}$ at 75.76 MHz can be fitted with two Lorentzian functions (Figure 9), corresponding to the aromatic and the aliphatic deuterons. On the other hand, two Lorentzian functions are not adequate in fitting the $(PS)_{92}$-*b*-$(PS\text{-}d_8)_{4.5}$-*b*-$(PS)_{17}$-*b*-$(PANa)_{15}$ block ionomer spectrum. A third Lorentzian function is needed to account for the broad component (Figure 10). The line widths obtained from the curve fitting procedure are also given in Table 3. These results clearly indicate that upon the micelle formation, a large fraction of the ^{2}H-labeled segments become less mobile. At 21 °C, the less mobile fraction accounts for 84% of the total signal, but this fraction decreases with increasing temperature, and at 70 °C, 56% of the signal belongs to the less mobile fraction.

Table 3. ^{2}H Relaxation Data for $(PS)_{92}$-*b*-$(PS\text{-}d_8)_{4.5}$-*b*-$(PS)_{17}$-*b*-$(PtBuA)_{15}$ measured at 76.75 MHz (11.75 T) and 30.70 MHz (4.70 T)

temp, °C	T_1 (11.75 T), ms aromatic	T_1 (11.75 T), ms aliphatic	$\Delta\nu_{1/2}$(11.75 T), Hz aromatic	$\Delta\nu_{1/2}$(11.75 T), Hz aliphatic	T_1(4.70 T), ms aromatic	T_1(4.70 T), ms aliphatic
21	6.57	6.65	170	154	2.84	2.84
30	6.40	6.53	143	134	2.80	2.80
40	6.43	6.50	123	109	3.28	2.88
50	6.68	6.62	105	97.8	3.79	3.66
60	6.98	6.99	94.5	90.1	4.35	4.20
70	7.52	7.45	85.2	82.0	4.91	4.76

Table 4. Relaxation Data for $(PS)_{92}$-*b*-$(PS\text{-}d_8)_{4.5}$-*b*-$(PS)_{17}$-*b*-$(PANa)_{15}$ Measured at 76.75 MHz (11.75 T) and 30.7 MHz (4.70 T)

temp, °C	T_1(11.75 T), ms aromatic	T_1(11.75 T), ms aliphatic	$\Delta\nu_{1/2}$(11.75 T), Hz aromatic	$\Delta\nu_{1/2}$(11.75 T), Hz aliphatic	$\Delta\nu_{1/2}$(11.75 T), Hz broad component	T_1(4.70 T), ms aromatic	T_1(4.70 T), ms aliphatic
21	7.96	8.04	166 (9%)[a]	189 (7%)[a]	1309 (84%)[a]	3.10[b]	3.10[b]
30	7.76	7.69	185 (13%)	169 (7%)	1309 (80%)	3.00	3.00
40	7.57	7.69	183 (16%)	170 (9%)	1242 (75%)	3.05	3.05
50	7.50	7.65	184 (21%)	165 (12%)	1201 (67%)	3.35	3.16
60	7.57	7.43	162 (23%)	164 (15%)	1137 (62%)	3.75	3.64
70	7.75	7.59	157 (27%)	149 (17%)	1173 (56%)	4.28	4.03

[a] The values given in parentheses are the weight fractions of the components, obtained from a least-squares fitting of Lorentzian functions; see Figure 6. [b] At 4.70 T, the ^{2}H signals from aromatic and aliphatic segments cannot be resolved at low temperatures.

Table 5. Correlation Times and Width Parameter (p) for $(PS)_{92}$-*b*-$(PS\text{-}d_8)_{4.5}$-*b*-$(PS)_{17}$-*b*-$(PtBuA)_{15}$ and $(PS)_{92}$-*b*-$(PS\text{-}d_8)_{4.5}$-*b*-$(PS)_{17}$-*b*-$(PANa)_{15}$ in CCl_4, Based on the Log χ^2 Distribution Model

	$(PS)_{92}$-*b*-$(PS\text{-}d_8)_{4.5}$-*b*-$(PS)_{17}$-*b*-$(PtBuA)_{15}$				$(PS)_{92}$-*b*-$(PS\text{-}d_8)_{4.5}$-*b*-$(PS)_{17}$-*b*-$(PANa)_{15}$			
	aromatic		aliphatic		aromatic		aliphatic	
temp, °C	τ_0, ns	p	τ_0, ns	p	τ_0, ns	p	τ_0, ns	p
21	1.7	21	1.7	21	3.8	12	4.0	12
30	1.5	23	1.5	22	3.2	13	3.1	13
40	1.0	24	1.3	23	2.6	13	2.6	13
50	0.66	27	0.72	25	1.6	13	1.7	13
60	0.50	30	0.51	29	0.94	14	1.1	14
70	0.39	31	0.42	30	0.58	17	0.64	17

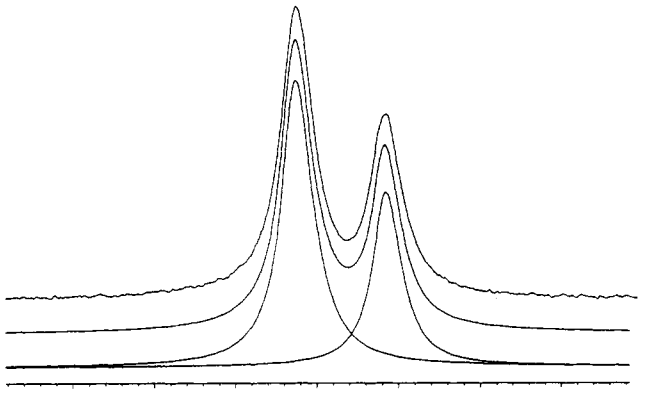

Figure 9. ^{2}H NMR spectrum (76.75 MHz) of $(PS)_{92}$-*b*-$(PS\text{-}d_8)_{4.5}$-*b*-$(PS)_{17}$-*b*-$(PtBuA)_{15}$ in CCl_4 (9.1% (w/w)) at 21 °C, fitted with Lorentzian functions.

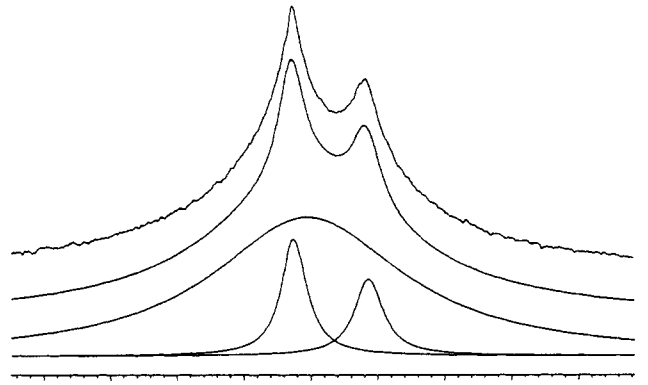

Figure 10. ^{2}H NMR spectrum (76.75 MHz) of $(PS)_{92}$-*b*-$(PS\text{-}d_8)_{4.5}$-*b*-$(PS)_{17}$-*b*-$(PANa)_{15}$ in CCl_4 (9.1% (w/w)) at 21 °C, fitted with Lorentzian functions.

The spin–lattice relaxation times of $(PS)_{92}$-*b*-$(PS\text{-}d_8)_{4.5}$-*b*-$(PS)_{17}$-*b*-$(PtBuA)_{15}$ and $(PS)_{92}$-*b*-$(PS\text{-}d_8)_{4.5}$-*b*-$(PS)_{17}$-*b*-$(PANa)_{15}$ were interpreted by use of the log χ^2 model and the results are given in Table 5. As the temperature increases, the mobility of ^{2}H-labeled segments is expected to increase. For both polymer systems, the rotational correlation time, τ_0, indeed decreases and the p value, which describes the width of the distribution of correlation times, increases with increasing temperature. In contrast, going from the nonionic precursor $(PS)_{92}$-*b*-$(PS\text{-}d_8)_{4.5}$-*b*-$(PS)_{17}$-*b*-$(PtBuA)_{15}$ to the block ionomer $(PS)_{92}$-*b*-$(PS\text{-}d_8)_{4.5}$-*b*-$(PS)_{17}$-*b*-$(PANa)_{15}$, the rotational correlation times increase and the p values decrease significantly at the temperature range studied, indicating slower motion in the block ionomer micelles. The spin–lattice relaxation data are consistent with the discussion of the previous sections based on line width and signal intensity.

Conclusions

The mobility of the soluble blocks in the coronas of poly(styrene-*b*-sodium acrylate) block ionomer micelles was probed at the segmental level by ^{2}H NMR. ^{2}H-labeled styrene segments (3–5 repeat units) were positioned at 0, 11, 14, 17, 20, 25, 50, and 74 styrene repeat units away from the nonionic–ionic block junction. It was found that the mobility of ^{2}H-labeled styrene segments close to the micellar cores is reduced significantly. The effect of micellization on mobility decreases as the distance between the ^{2}H-labeled styrene segments and the nonionic–ionic block junction increases. Styrene segments 20 repeat units away from the nonionic–ionic block junction can still "feel" the restriction imposed by the ionic cores. However, this restriction disappears completely when PS segments are 50 repeat units away from the nonionic–ionic block junction.

The effect of ionic interaction on mobility in sodium carboxylate terminated polystyrene ionomers was also investigated. The dependence of mobility on the distance between the ionic groups and the ^{2}H-labeled segments is similar to that of block ionomers. It is of special interest to observe that the presence of only one terminal ionic group can impose restriction on the dynamics of ^{2}H-labeled styrene located 14 repeat units away from the point of attachment. It is anticipated that for the soluble blocks in ionomer solution and the nonionic segments in ionomer above its matrix T_g, the effect of ionic association on chain dynamics is similar in trend. Thus, the present result is in support of the recent ionomer model proposed by Eisenberg, Hird, and Moore, which is based on the mobility reduction in the vicinity of ionic multiplets.[35]

The length of the ionic block was also found to have a substantial effect on the dynamics of the soluble segments, especially when the ionic block is shorter than 6 sodium acrylate units. When the ionic block length is longer than 6 sodium acrylate units, this effect on the ^{2}H-labeled styrene segments 14 repeat units away become less significant. Spin–lattice relaxation times at multiple fields and multiple temperatures were also measured for $(PS)_{92}$-*b*-$(PS\text{-}d_8)_{4.5}$-*b*-$(PS)_{17}$-*b*-$(PtBuA)_{15}$ and $(PS)_{92}$-*b*-$(PS\text{-}d_8)_{4.5}$-*b*-$(PS)_{17}$-*b*-$(PANa)_{15}$, and the results were interpreted by means of the log χ^2 distribution model. Compared to the nonionic precursor, the average correlation time of the ionomer is much longer and the distribution of correlation times is broader.

Added in Proof: The collective dynamics of tethered chains was investigated recently by Farago et al. for polystyrene (PS)–polyisoprene (PI) diblock copolymers in *n*-decane, using neutron spin–echo spectroscopy.[73] It was found that the dynamic response from PI single chains in dilute solution is completely different from that of the PI chains within the corona. This was explained using a model based on the idea of de Gennes for treating the corona as a semidilute polymer solution with varying concentration profile.

Acknowledgment. Funding for this research from the National Sciences and Engineering Research Council of Canada (NSERC) is acknowledged.

References and Notes

(1) Riess, G.; Hurtrez, G.; Bahadur, P. In *Encyclopedia of Polymer Science and Engineering*, 2nd ed.; John Wiley & Sons: New York, 1985; Vol. 2, p 324.
(2) Halperin, A.; Tirrell, M.; Lodge, T. P. *Adv. Polym. Sci.* **1992**, *100*, 31.
(3) Brown, R. A.; Masters, A. J.; Price, C.; Yuan, X. F. In *Comprehensive Polymer Science*; Booth, C., Price, C., Ed.; Pergamon Press: Toronto, 1989; Vol. 2, p 155.
(4) Price, C. In *Development in Block Copolymers*; Goodman, I., Ed.; Elsevier Applied Science: London, 1982; Vol. 1, Chapter 2.
(5) Selb, J.; Gallot, Y. In *Development in Block Copolymers*; Goodman, I., Ed.; Elsevier Applied Science: London, 1985; Vol. 2, Chapter 2.
(6) Tuzar, Z.; Kratochvil, P. *Adv. Colloid Interface Sci.* **1976**, *6*, 201.
(7) Tuzar, Z. *Macromol. Rep.* **1992**, *A29* (Suppl. 2), 173.
(8) Nakamura, K.; Endo, R.; Takeda, M. *J. Polym. Sci., Polym. Phys. Ed.* **1977**, *15*, 2087.
(9) Heatley, F.; Begum, A. *Makromol. Chem.* **1977**, *178*, 1205.
(10) Spevacek, J. *Makromol. Chem., Rapid Commun.* **1982**, *3*, 697.
(11) Candau, F.; Heatley, F.; Price, C.; Stubbersfield, R. B. *Eur. Polym. J.* **1984**, *20*, 685.
(12) Waggoner, A. S.; Griffith, O. H.; Christenson, C. R. *Proc. Natl. Acad. Sci. U.S.A.* **1967**, *57*, 1198.
(13) Yeung, A. S.; Frank, C. W. *Polymer* **1990**, *31*, 2101.

(14) Wilhelm, M.; Zhao, C.-L.; Wang, Y.; Xu, R.; Winnik, M. A. *Macromolecules* **1991**, *24*, 1033.
(15) Prochazka, K.; Kiserow, D.; Ramireddy, C.; Tuzar, Z.; Munk, P.; Webber, S. E. *Macromolecules* **1992**, *25*, 454.
(16) Vagberg, L. J. M.; Cogan, K. A.; Gast, A. P. *Macromolecules* **1991**, *24*, 1670.
(17) Cogan, K. A.; Gast, A. P.; Capel, M. *Macromolecules* **1991**, *24*, 6512.
(18) Zhu, J.; Eisenberg, A.; Lennox, R. B. *J. Am. Chem. Soc.* **1991**, *113*, 5583.
(19) Zhu, J.; Lennox, R. B.; Eisenberg, A. *J. Phys. Chem.* **1992**, *96*, 4727.
(20) Desjardins, A.; Eisenberg, A. *Macromolecules* **1991**, *24*, 5779.
(21) Desjardins, A.; van de Ven, T. G. M.; Eisenberg, A. *Macromolecules* **1992**, *25*, 2412.
(22) Gao, Z.; Desjardins, A.; Eisenberg, A. *Macromolecules* **1992**, *25*, 1300.
(23) Zhong, X. F.; Varshney, S. K.; Eisenberg, A. *Macromolecules* **1992**, *25*, 7160.
(24) Cao, T.; Munk, P.; Ramireddy, C.; Tuzar, Z.; Webber, S. E. *Macromolecules* **1991**, *24*, 6300.
(25) Kiserow, D.; Prochazka, K.; Ramireddy, C.; Tuzar, Z.; Munk, P.; Webber, S. E. *Macromolecules* **1992**, *25*, 461.
(26) Ramireddy, C.; Tuzar, Z.; Prochazka, K.; Webber, S. E.; Munk, P. *Macromolecules* **1992**, *25*, 2541.
(27) Khougaz, K.; Gao, Z.; Eisenberg, A. To be published.
(28) Holliday, L., Ed. *Ionic Polymers*; Applied Science Publishers: London, 1975.
(29) Eisenberg, A.; King, M. *Ion-Containing Polymers, Physical Properties and Structure*; Academic Press: New York, 1977.
(30) MacKnight, W. J.; Earnest, T. R., Jr. *J. Polym. Sci., Macromol. Rev.* **1981**, *16*, 41.
(31) Pineri, M.; Eisenberg, A., Eds. *Structure and Properties of Ionomers*; NATO Advanced Study Institute Series 198; D. Reidel Publishing Co.: Dordrecht, Holland, 1987.
(32) Tant, M. R.; Wilkes, G. L. *J. Macromol. Sci., Rev. Macromol. Chem. Phys.* **1988**, *C28*, 1.
(33) Mauritz, K. A. *J. Macromol. Sci., Rev. Macromol. Chem. Phys.* **1988**, *C28*, 65.
(34) Fitzgerald, J. J.; Weiss, R. A. *J. Macromol. Sci., Rev. Macromol. Chem. Phys.* **1988**, *C28*, 99.
(35) Eisenberg, A.; Hird, B.; Moore, R. B. *Macromolecules* **1990**, *23*, 4098 and references therein.
(36) Grest, G. S.; Kremer, K.; Witten, T. A. *Macromolecules* **1987**, *20*, 1376.
(37) Grest, G. S.; Kremer, K.; Milner, S. T.; Witten, T. A. *Macromolecules* **1989**, *22*, 1904.
(38) Naylor, A. M.; Goddard, W. A., III. *Polym. Prepr. (Am. Chem. Soc., Div. Polym. Chem.)* **1988**, *29*, 215.
(39) Lescanec, R.; Muthukumar, M. *Macromolecules* **1990**, *23*, 2280.
(40) Daoud, M.; Cotton, J. P. *J. Phys. Fr.* **1982**, *43*, 531.
(41) Roovers, J.; Hadjichristidis, N.; Fetters, L. J. *Macromolecules* **1983**, *16*, 214.
(42) Huber, K.; Burchard, W.; Fetters, L. *J. Macromolecules* **1984**, *17*, 541.
(43) Khasat, N.; Pennisi, R. W.; Hadjichristidis, N.; Fetters, L. J. *Macromolecules* **1988**, *21*, 1100.
(44) Lantman, C. W.; MacKnight, W. J.; Rennie, A. R.; Tassin, J. F.; Monnerie, L.; Fetters, L. J. *Macromolecules* **1990**, *23*, 836.
(45) Fetters, L. J.; Kiss, A. D.; Pearson, D. S.; Quack, G. F.; Vitus, F. J. *Macromolecules* **1993**, *26*, 647.
(46) Meltzer, A. D.; Tirrell, D. A.; Jones, A. A.; Inglefield, P. T.; Hedstrand, D. M.; Tomalia, D. A. *Macromolecules* **1992**, *25*, 4541.
(47) Meltzer, A. D.; Tirrell, D. A.; Jones, A. A.; Inglefield, P. T. *Macromolecules* **1992**, *25*, 4549.
(48) Cosgrove, T. *J. Chem. Soc., Faraday Trans.* **1990**, *86* (9), 1323.
(49) Cosgrove, T.; Griffiths, P. C. *Adv. Colloid Interface Sci.* **1992**, *42*, 175.
(50) Cosgrove, T. *Macromol. Rep.* **1992**, *A29* (Suppl. 2), 125.
(51) Chachaty, C. *Prog. Nucl. Magn. Reson. Spectrosc.* **1986**, *19*, 183.
(52) Martin, C. A.; Magid, L. J. *J. Phys. Chem.* **1981**, *85*, 3938.
(53) Carnali, J.; Lindman, B.; Soderman, O.; Walderhaug, H. *Langmuir* **1986**, *2*, 51.
(54) Wennerstrom, H.; Lindman, B.; Soderman, O.; Drakenberg, T.; Rosenholm, J. B. *J. Am. Chem. Soc.* **1979**, *101*, 8860.
(55) Abragam, A. *The Principles of Nuclear Magnetism*; Clarendon Press: Oxford, U.K., 1961.
(56) Bloembergen, N.; Purcell, E. M.; Pound, R. V. *Phys. Rev.* **1948**, *73*, 679.
(57) Bovey, F. A.; Jelinski, L. W. *J. Phys. Chem.* **1985**, *89*, 571.
(58) Kitamaru, R. In *Applications of NMR Spectroscopy to Problems in Stereochemistry and Conformation Analysis*; Kakeuchi, Y., Marchand, A. P., Eds.; VCH: Deerfield Beach, FL, 1986; p 75.
(59) Heatley, F. *Annu. Rep. NMR Spectrosc.* **1986**, *17*, 179.
(60) Lipari, G.; Szabo, A. *J. Am. Chem. Soc.* **1982**, *104*, 4546.
(61) Lipari, G.; Szabo, A. *J. Am. Chem. Soc.* **1982**, *104*, 4559.
(62) Dejean de la Batie, R.; Laupretre, F.; Monnerie, L. *Macromolecules* **1988**, *21*, 2045.
(63) Dejean de la Batie, R.; Laupretre, F.; Monnerie, L. *Macromolecules* **1988**, *21*, 2052.
(64) Gisser, D. J.; Glowinlowski, S.; Ediger, M. D. *Macromolecules* **1991**, *21*, 4270.
(65) Radiotis, T.; Brown, G. R.; Dais, P. *Macromolecules* **1993**, *26*, 1445.
(66) Schaefer, J. *Macromolecules* **1973**, *6*, 882.
(67) Hautekeer, J. P.; Varshney, S. K.; Fayt, R.; Jacobs, C.; Jerome, R.; Tessie, Ph. *Macromolecules* **1990**, *23*, 3893.
(68) Gao, Z.; Zhong, X. F.; Morin, F. G.; Eisenberg, A. To be published.
(69) Hird, B.; Eisenberg, A. *J. Polym. Sci., Polym. Phys. Ed.* **1990**, *28*, 1665.
(70) Williams, C. E.; Russell, T. P.; Jerome, R.; Horrion, J. *Macromolecules* **1986**, *19*, 2877.
(71) Halperin, A. *Macromolecules* **1987**, *20*, 2943.
(72) Blum, F. D.; Sinha, B. R.; Schwab, F. C. *Macromolecules* **1990**, *23*, 3592.
(73) Farago, B.; Monkenbusch, M.; Richter, D.; Huang, J. S.; Fetters, L. J.; Gast, A. P. *Phys. Rev. Lett.* **1993**, *71*, 1015.